communications biology

Article

https://doi.org/10.1038/s42003-024-06929-5

Dual spatial host-bacterial gene expression in *Mycobacterium abscessus* respiratory infections

Federico Di Marco[1,2,3,5], Francesca Nicola[1,4,5], Francesca Giannese[3], Fabio Saliu[1], Giovanni Tonon[3], Stefano de Pretis[3,6], Daniela M. Cirillo[1,6] & Nicola I. Lorè[1,6]

Co-localization of spatial transcriptome information of host and pathogen can revolutionize our understanding of microbial pathogenesis. Here, we aimed to demonstrate that customized bacterial probes can be successfully used to identify host-pathogen interactions in formalin-fixed-paraffin-embedded (FFPE) tissues by probe-based spatial transcriptomics technology. We analyzed the spatial gene expression of bacterial transcripts with the host transcriptomic profile in murine lung tissue chronically infected with *Mycobacterium abscessus* embedded in agar beads. Customized mycobacterial probes were designed for the constitutively expressed *rpoB* gene (an RNA polymerase β subunit) and the virulence factor precursor *lsr2*, modulated by oxidative stress. We found a correlation between the *rpoB* expression, bacterial abundance in the airways, and an increased expression of *lsr2* virulence factor in lung tissue with high oxidative stress. Overall, we demonstrate the potential of dual bacterial and host gene expression assay in FFPE tissues, paving the way for the simultaneous detection of host and bacterial transcriptomes in pathological tissues.

High-resolution technologies are improving our understanding of the complex dynamics of infection processes[1–5]. Current approaches lack the simultaneous co-localization of spatial biological information between the host environment and the expression of bacterial virulence factors. Moreover, little information is available on the pathogen's gene expression and spatial location during infection[6–12]. Few recent studies have shown the spatial localization of bacteria in tissues in the context of host transcriptome profiles[9,10]. Recent progresses have been made in the study of host-virus interaction[1,11], little is known on the expression of specific bacterial virulence genes during infection in pathological tissues. Recent studies related to the spatial localization of bacteria in tissues were limited to the quantification of microbial taxa without providing information on the gene expression profile in individual microbial cells in relation to host transcriptome profiles[9,10]. A recent methods based on spatial meta-transcriptomics resolves host-bacteria-fungi interactomes, although this approach lacks the detection of bacterial transcriptomic profiles[12]. In addition, the potential of an imaging-based approach, i.e., highly multiplexed spatial transcriptomics, was recently shown. The authors profiled cultured bacteria in a wide range of biological and spatial contexts, highlighting the heterogeneity of their gene expression profiles[13].

So far, several technical limitations, such as poor permeabilization of the bacterial membrane, lack of polyadenylation of bacterial messenger RNA, and low abundance and stability of bacterial messenger RNA encoding virulence, have hampered the study of bacterial gene expression in tissues using omics technologies[6–8,10,14,15]. Current spatial transcriptomic technologies have the potential to overcome these issues by exploiting probe-based strategies to improve the detection of specific RNA transcripts (e.g., those with low abundance or low stability)[16]. In addition, probe-based methods are compatible with formalin-fixed paraffin-embedded (FFPE) tissue blocks, allowing easy access to infected material and to large amounts of samples already deposited in biobanks[16].

Here, we hypothesize that existing technological approaches could be adapted to identify the spatial distribution of bacteria and detect virulence factors affected by interactions with inflammatory tissue environments, and vice versa. Among bacterial pathogens, *Mycobacterium abscessus* (*M. abscessus*) is an emerging ubiquitous multidrug-resistant microorganism[17,18] that can cause a variety of clinical syndromes/diseases, including the clinical manifestation of non-tuberculous mycobacteria (NTM) lung disease[19]. In NTM disease, it is often unclear whether the pathological outcome in the

[1]Emerging Bacterial Pathogens Unit, Division of Immunology, Transplantation and Infectious, IRCCS Ospedale San Raffaele, Milan, Italy. [2]Department of Informatics, Systems and Communication, Università degli Studi di Milano-Bicocca, Milan, Italy. [3]Center for Omics Sciences, IRCCS Ospedale San Raffaele, Milan, Italy. [4]Università Vita-Salute San Raffaele, Milan, Italy. [5]These authors contributed equally: Federico Di Marco, Francesca Nicola. [6]These authors jointly supervised this work: Stefano de Pretis, Daniela M. Cirillo, Nicola I. Lorè. e-mail: lore.nicolaivan@hsr.it

lung is mediated by the response to *M. abscessus* or by the altered inflammatory microenvironment itself.

Therefore, to investigate simultaneously the spatially-resolved host and bacterial transcriptional profiles, we employed the probe-based assay (Visium Spatial Gene Expression assay) on FFPE tissue blocks at a resolution of 55 µm (Fig. 1A, B). We were interested in mycobacterial lung infection, with particular attention to *M. abscessus*[17]; indeed, we utilized tissue blocks from animals chronically infected with *M. abscessus* embedded in agar beads[20,21], as a disease model. To prove the dual spatial gene expression of bacteria and host in tissues, we designed custom probes focusing on two specific mycobacterial transcripts: a constitutive expressed gene, named *rpoB*, that encode for the RNA polymerase β subunit[22], and a

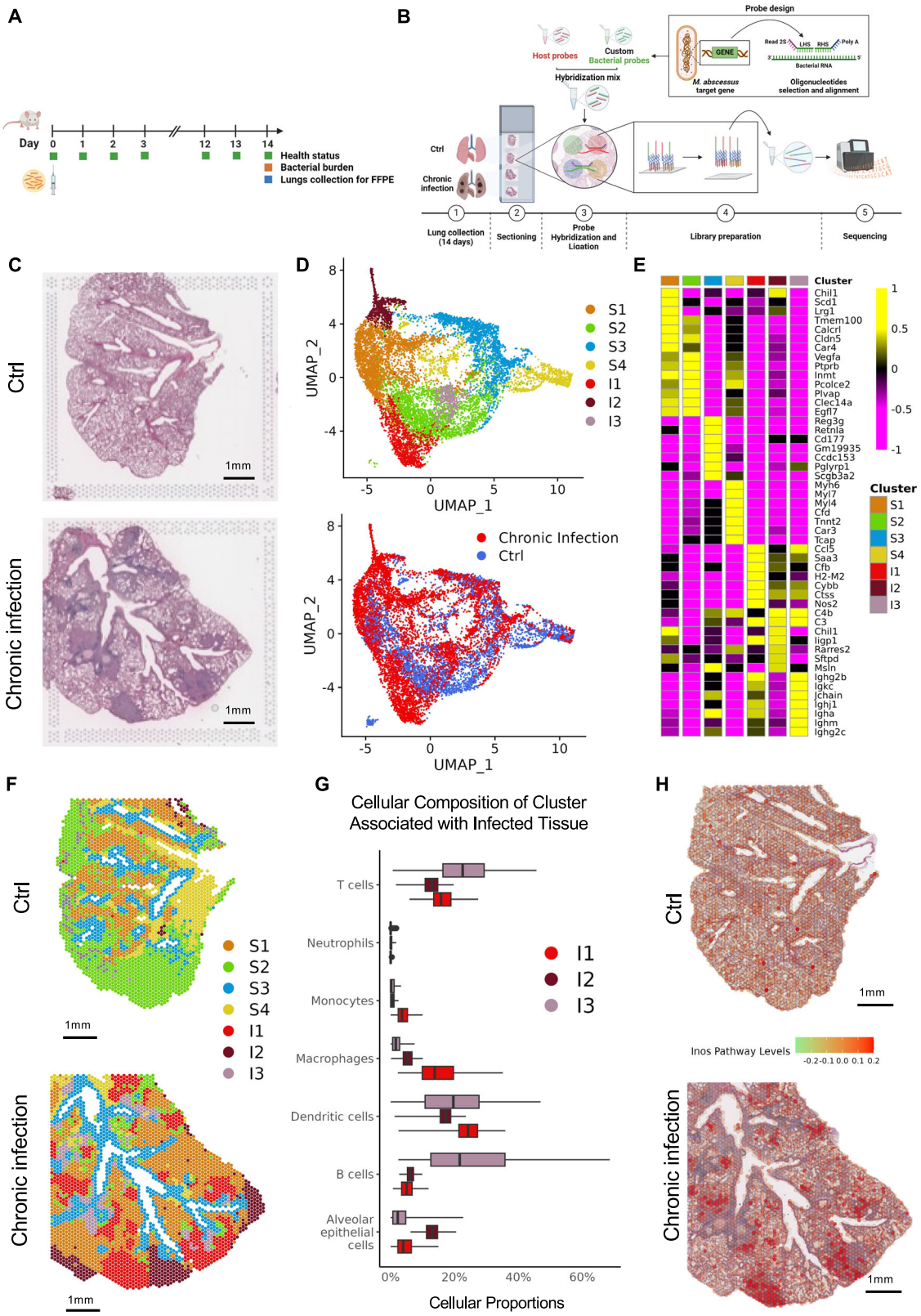

Fig. 1 | Transcriptional and spatial analysis of not-infected (Ctrl) and chronically infected lungs (Chronic infection). A Schematic representation of a mouse model of infection (Created in BioRender. Tonon, G. (2024) BioRender.com/d23x524). **B** Schematic representation of the spatial transcriptomic experiment. (Created in BioRender. Tonon, G. (2024) BioRender.com/d23x524) **C**) H&E staining of Ctrl and chronically infected lungs used for spatial transcriptomic (Scale bar, 1 mm). **D** UMAP dimensionality plot of sequenced spots from "Ctrl" ($n = 2$) and "Chronic infection" ($n = 2$) slices, color-coded by transcriptional clusters (top) and case (bottom). **E** Heatmap showing the expression levels of the top seven transcriptional markers for each cluster, as identified by differential expression analysis. The color scale represents the average log2 fold change when comparing the cluster to the others. **F** Spatial dimensionality plot of "Ctrl" and "Chronic infection" slices, color-coded by transcriptional clusters as in (**D**). The spots are arranged according to their spatial coordinates in the tissue sections (Scale bar, 1 mm). **G** Boxplot showing the cellular composition distribution of inflammatory clusters (I1, I2, and I3) across "Chronic infection" ($n = 2$) slices. **H** Spatial plot showing the expression levels of the iNOS pathway module in "Ctrl" and "Chronic infection" slices (Scale bar, 1 mm).

well-known oxidative stress-modulated bacterial virulence factor precursor, called *lsr2*, which is responsible for encoding a nucleoid-associated protein (NAP)[23,24].

Using this innovative approach, we found that bacterial gene expression can vary in tissues in different inflammatory areas of the host. The results showed that both *rpoB* and *lsr2* transcripts were detectable and MABS+ areas (spots positive for the presence of *M. abscessus* transcripts) were associated with host inflammatory profiles, including immunoglobulin genes, inflammatory cytokines, macrophagic regulation, and antimicrobial response. Furthermore, *rpoB* expression was higher compared to *lsr2* gene expression and *lsr2* expression was associated with higher levels of the inducible-Nitric Oxide Synthase (iNOS) pathway, responsible for the host response to oxidative stress. The study demonstrates the effective use of a dual bacterial and host gene expression assay in FFPE tissues. Overall, our approach paves the way for the study of microbial pathogenesis in various bacterial diseases by simultaneously detecting the host and bacterial transcriptome in pathological tissues.

Results and discussion

Spatial host gene expression reveals different inflammatory states in lung tissue with chronic *M. abscessus* infection

We used a newly designed dual probe-based method for spatial host-pathogen gene expression (see "Methods") and exploited FFPE tissues from lung of mice displaying chronic infection by *M. abscessus* (ATCC 19977 strain)[17]. Chronic in vivo infection with *M. abscessus* was performed using an agar beads murine model. This approach can replicate bacterial persistence in aggregates and planktonic bacilli, which can potentially express diverse bacterial virulence factors as well as a wide range of inflammatory processes in the airways and parenchymal areas[20,25,26]. Mice were infected with an intratracheal injection of 10^5 colony-forming units (CFU) embedded in agar beads, allowing persistence in the lung of C57BL/6N mice with a sustained bacterial load (Fig. 1A). At 14 days post-challenge, these mice display a median bacterial load of around 4×10^6 CFU with a 100% incidence of chronic infection. In this mouse model, *M. abscessus* can persist from 7 to 90 days and is associated with granuloma-like structure areas in the lung, as previously published[27].

Therefore, to set up our dual spatial probe-based sequencing, we decided to consider FFPE tissues from one infected mouse ($n = 2$ slices) and one uninfected mouse ($n = 2$ slices) as negative control (Fig. 1A, B). The two consecutive infected lung slices revealed the histological profile associated with *M. abscessus* persistence, including inflammatory foci characterized by infiltrating macrophages or early granuloma-like structures (Fig. 1C, Supplementary Figs. 1 and 4).

The transcriptome profiles of the infected lung exhibited distinct expression patterns compared to the control mouse, as shown in the unsupervised cluster analysis (Fig. 1D–F, Supplementary Figs. 1, 2, and 3). Moreover, we identified a total of four clusters shared between control and infected mice (named S1, S2, S3, and S4), and three clusters located in the chronically Infected mouse (named I1, I2, and I3) (Fig. 1E, Supplementary Figs. 1, 2, and 3). Clusters located in chronically infected mice co-localized with pathological areas, including within (Cluster I1) or surrounding (Cluster I2) tissue with infiltrating macrophages/granuloma-like structures, or with submucosal inflammatory cells (Cluster I3), as observed in terms of H&E staining (Fig. 1F, Supplementary Figs. 1 and 4). Similar findings in terms of spatial distribution were confirmed by our dual spatial probe-based assay when different and consecutive FFPE tissue sections were analyzed for both groups (Supplementary Figs. 1, 2, and 3). We carried out a deconvolution approach to define the proportion of cell types for each spot in the four slices using the Robust Cell-Type Decomposition (RCTD) method[4,28], and an annotated single-cell RNAseq reference dataset from Xu et al.[4] (GEO: GSE190225) comprehending 12 cell types from mouse lung infected with *Klebsiella pneumoniae*. The deconvolution results were shown as proportions of 12 cell types in each cluster (Supplementary Fig. 5). Shared clusters (S1, S2, S3, and S4) were mainly composed of stromal cells, such as alveolar, club, endothelial, and fibroblast cells. In contrast, the three clusters within the chronically Infected mouse (I1, I2, and I3) displayed higher proportions of immune cells, including macrophage, monocyte, B, and T cells (Supplementary Fig. 5). Those cellular profiles were in line with Gene Ontology terms associated with cluster markers (Supplementary Figs. 5, 6 and Supplementary Data 1).

Following this, we focused our attention on cluster I1, which presented a high-level proportion of granuloma-associated cells, such as macrophages, dendritic cells, club cells, and T cells[5,29,30] (Fig. 1G). To further confirm the host spatial molecular characterization of the I1 cluster, we determined the spatial distribution of gene expression markers (selected from Gene Ontology terms) associated with host response to *M. abscessus*, such as the iNOS or reactive oxygen species (ROS) pathways. We confirmed that the signal level of both iNOS and ROS pathways were upregulated in the infected mouse compared with the control group (Supplementary Figs. 7 and 8) and co-localized with the granuloma-like structure, as shown in Fig. 1H and Supplementary Figs. 4, 5, and 6.

Spatial bacterial gene expression detects microbial expression patterns in lungs with chronic *M. abscessus* infection

Next, we determined the feasibility of assaying bacterial and host probes in the same tissue section using our dual spatial probe-based sequencing approach. In addition to the 18k host gene targeted by the commercial kits, we designed and developed 3 pairs of custom probes per gene, targeting two distinct bacterial transcripts. We were interested in showing the effectiveness of this approach in mycobacterial infection, with particular attention to *M. abscessus*. Therefore, we focused on two distinct mycobacterial transcripts: one constitutive expressed gene, named *rpoB*[22], and a well-known precursor of bacterial virulence factor modulated by oxidative stress, referred to as *lsr2*[23,24]. We also refined the Visium protocol by incorporating our new probes into the modified permeabilization protocol to improve probe hybridization due to the mycobacterial membranes (see "Methods"). The expression of the selected bacterial targets, *rpoB* and *lsr2*, was spatially detected (Fig. 2A and Supplementary Fig. 9). To validate the detection obtained with our *M. abscessus* probes, we compared *M. abscessus* localization by spatial transcriptomics assay with *M. abscessus* detection assays by orthogonal Kinyoun Stain (Supplementary Fig. 9) and ad hoc immunofluorescence staining (Fig. 2B) on consecutive tissue sections. We observed that airways and submucosal airway areas displayed a higher number of bacteria (Fig. 2A I) compared to parenchymal or granuloma-like structure areas (Fig. 2A II, III) of uninfected control regions (Fig. 1A IV) and control mouse (Supplementary Fig. 10). Overall, these results demonstrate that the selected bacterial probes and the refined protocol can be used to detect bacterial transcripts in infected organs co-localized with host transcriptome profiles.

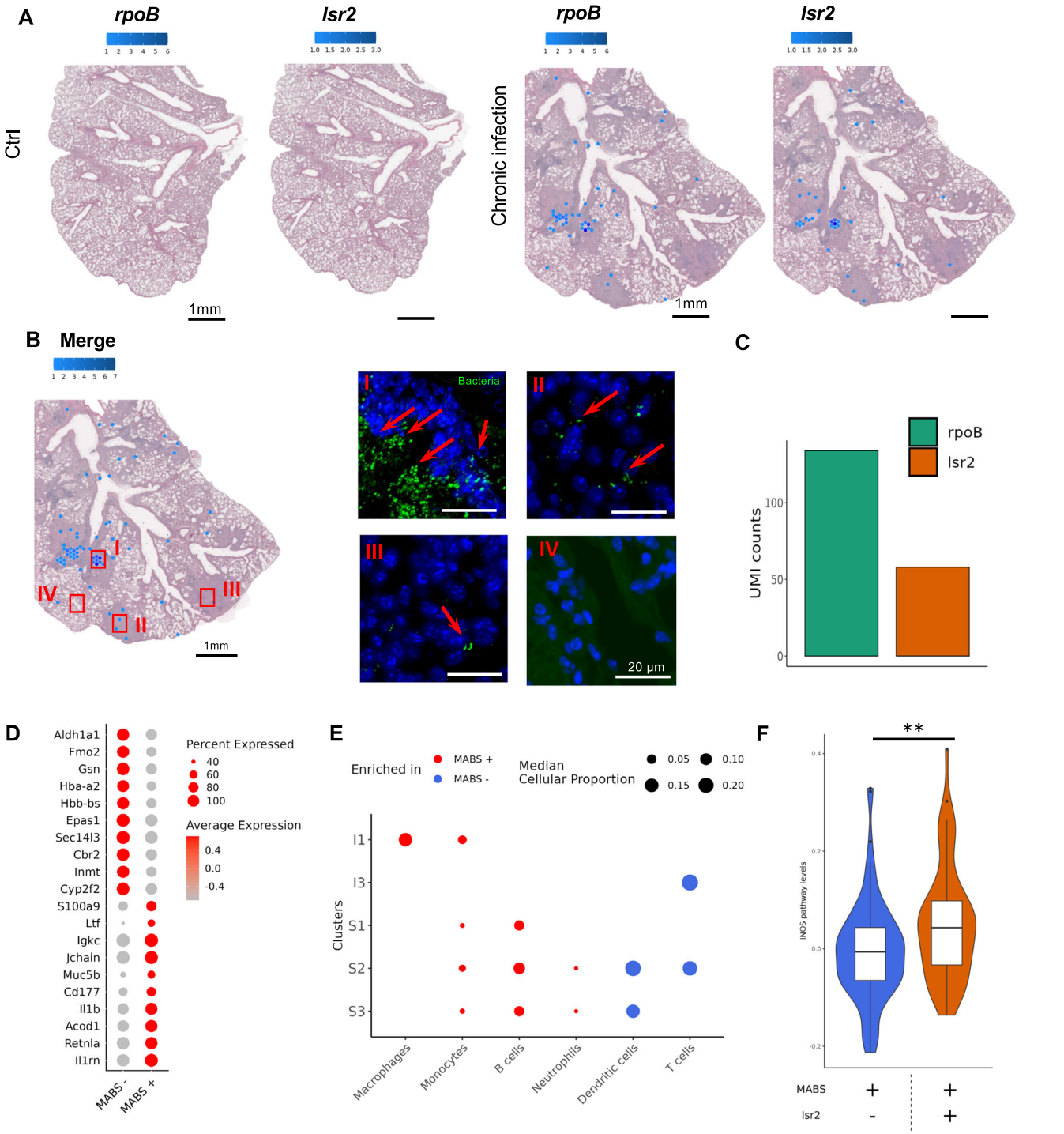

Fig. 2 | Spatial and quantitative analysis of *rpoB* and *lsr2* probes in Ctrl and Chronic infection slices. A Spatial plot showing the UMI counts of *rpoB* and *lsr2* probes in "Ctrl" and "Chronic infection" representative slices. The color scale indicates the number of UMIs per spot (Scale bar, 1 mm). **B** Spatial plot showing the summed UMI counts of *rpoB* and *lsr2* probes in "Chronic infection" slices ($n = 2$). The color scale indicates the total number of UMIs per spot (Scale bar, 1 mm). (I–IV) Representative images of immunofluorescence staining in infected mouse for *M. abscessus* (with specific antibody against *M. abscessus*, stained in green, and with Hoechst 33342, Trihydrochloride, stained in blue) in airways and submucosal airways (**B** I), in granuloma-like structure areas (**B** II, III), and area of not inflamed parenchyma (**B** IV) all captured in the successive slice of the infected sample used for spatial transcriptomics (Scale bar, 20 µm). **C** Barplot showing the gathered UMI counts of *rpoB* and *lsr2* probes in "Chronic infection" slices. The y-axis shows the number of UMIs. The bars are color-coded by the respective probe. **D** Bubble plot showing the differentially expressed genes in MABS+ (positive) and MABS− (negative) spots in "Chronic infection" slices ($n = 2$). The color scale shows the log fold change of the genes. The size of the bubbles indicates the percentage of spots expressing a gene. **E** The bubble plot illustrates the significantly different cellular populations between MABS+ (positive) and MABS− (negative) spots, categorized by clusters. Red dots indicate enrichment in MABS-positive spots, while blue dots indicate enrichment in MABS-negative spots. The size of each dot corresponds to the median cellular proportion observed for the specific cluster. **F** Violin plot for the levels of iNOS pathway grouped according to MABS+lsr2- or MABS+lsr2+ infection (generated with "Chronic infection" slices, $n = 2$) (Mann–Whitney test, $^{**}p$-value < 0.01).

Dual spatial host bacterial gene expression reveals *M. abscessus* and its virulence factor *lsr2* are associated with different inflammatory states in lung chronic infection

Next, we investigated the distribution of *M. abscessus* transcripts profile in the two consecutive tissue sections from the infected mouse. In these sections, 2.15% of spots had an *M. abscessus* transcriptional signal (MABS+ areas, with positive spots for the presence of either *rpoB* or *lsr2* or both transcripts), with highly reproducible capture of *M. abscessus* gene spots (67 and 63 bacterial spots out of 3176 and 2875 total spots in slice C1 and D1, respectively) (Supplementary Fig. 9A). In addition, we found that UMI counts were higher for the constitutively expressed *rpoB* gene than for the *lsr2* gene, and the overall numbers were similar between two different sections (Fig. 2C and Supplementary Fig. 11A).

Our approach allowed us to perform dual spatial host and *M. abscessus* gene expression analysis to identify changes in host gene expression induced by bacterial presence in lung cells at a resolution of 55 µm. We compared host gene expression patterns between the *M. abscessus* positive (MABS+, positive spots for the presence of *M. abscessus* transcripts) and negative (MABS−, negative spots for *M. abscessus* transcripts) spots. In the top 10 up- and down-regulated genes, we found upregulation of a specific immunoglobulin gene (*Igkc*), inflammatory cytokines (*Il1b* and *Il1rn*), macrophagic regulation (*Retnla* and *Acod1*) as well as neutrophilic (*Cd177*) and antimicrobial response (*S100a9*) in the MABS+ spots (Fig. 2D) (differential expression analysis used the Mann–Whitney test, p-value < 0.05). In addition, we compared cellular composition associated with MABS+ and MABS− spots among clusters (Fig. 2E, see "Methods"). MABS+ spots were significantly enriched in Macrophages and Monocytes within Cluster I1, co-localized with granuloma-like structures, while Monocytes, B cells, and Neutrophils were mainly enriched in MABS+ spots within Cluster S1, S2 and S3. Only Dendritic and T cell proportions were mainly present in MABS − spots within I3, S2, and S3 clusters (Fig. 2E).

Moreover, we hypothesized that bacterial probes targeting either a constitutively expressed gene, *rpoB*[22], or a bacterial virulence factor precursor, *lsr2*, may differently be expressed in diverse host inflammatory areas. As mentioned, *Isr2* is a virulence factor precursor critical for *M. abscessus* in oxidative stress condition and for macrophage internalization in mycobacterial infection[23,24,31]. Therefore, we determined whether diverse host tissue immune responses (e.g., lung areas with different oxidative stress states) in the bacterial positive spots (MABS+) could influence the expression of *lsr2* transcripts differently. When we examined spatial gene expression in the infected lung related to oxidative stress processes, such as the nitric oxide biosynthetic pathway, we confirmed that the *lsr2*+ positive spots among MABS+ spots (MABS+ *lsr2*+) were significantly enriched in the expression of iNOS pathways than lsr2- negative spots (MABS+ *lsr2*-) (Fig. 2F, adjusted $p < 0.01$ and Supplementary Fig. 11B). Overall, we confirmed that lung areas with high oxidative stress conditions were co-localized with the expression of the *lsr2* virulence factor precursor.

Conclusions

Our results show that bacterial probes are suitable for the spatial localization of bacteria in inflamed and not-inflamed lung tissues. Moreover, our study highlights the power of this method for detecting bacteria and their virulence factors under modulation by the local host environment, such as mycobacterial *lsr2* expression and the inducible nitric oxide host response. In addition, thanks to our approach and data on virulence factor precursor expression of the *lsr2* gene in pathological tissue, we can confirm its relevance both as a potential vaccine candidate against *M. abscessus* infection and as well as a bacterial target required for productive mycobacteriophage infection, as already published[23,24,32]. Defining the interaction between *M. abscessus* and the lung regarding the organization and spatial distribution of bacteria and infected niches is needed in treatment decision-making, requiring a deeper understanding of the complex mycobacterial-host interactions in pathological tissues and associated lung diseases.

Our approach deciphers the simultaneous and spatially distributed expression of mycobacterial and host genes in tissues and can decode the spatial pathological complexity of chronic lung disease caused by *M. abscessus* interactions. This study evidence supports that our approach is consistent and can be scaled up to target several bacterial transcripts. Moreover, our data suggest that *M. abscessus* can be associated with specific cell types based on tissue spatial localization, such as the mucosal barrier or within granuloma-like structures. Therefore, increasing the number of biological replicates and scaling up the bacterial probes could allow for a more accurate dissection of cell type/bacteria interactions, including specific host gene expression patterns associated with bacteria. In the future, using pools of probes targeting the overall *M. abscessus* transcriptome we will assess the diverse bacterial population states within distinct geographical areas of the mouse lung, simultaneously with host transcriptomic profiling. In addition, an increased number of biological replicates and a deeper sequencing of the bacterial probes will highlight differences in spatial localization among bacterial transcripts. Our custom approach, based on the design of a unique set of probes to define specific bacterial transcriptome profiles, is not limited to mycobacterial infections. In fact, it can be broadly applied to other infectious agents affecting the lung or other organs, such as *Pseudomonas aeruginosa*, *Klebsiella pneumoniae*, *Salmonella enterica typhi*, among others. In conclusion, our results demonstrate the power of the dual host-bacterial gene expression assay for studying microbial pathogenesis in various bacterial diseases and pave the way for future research on how inflammatory environments modulate pathogen virulence and vice versa.

Methods

Mouse models of chronic *M. abscessus* infection

We used a recently refined mouse model of respiratory infection by *M. abscessus*, exploiting C57BL/6 mice and agar beads[20,21,26,27,33,34]. The agar beads method was used to establish a stable infection in mice and reproduce a chronic infection faithfully. Specifically, *M. abscessus* was inoculated at 37 °C in a bacterial incubator shaker (200RPM) for two days (up to exponential phase) in 20 mL of Middlebrook 7H9 broth enriched with OADC. The resulting bacterial suspension was then concentrated to an optical density (OD) of 25 in 1 mL of DPBS and used to prepare the beads. After that, 25 mL of trypticase soy agar (TSA) and 50 mL of white heavy mineral oil were added to the bacterial suspension and mixed at medium speed with a magnetic stirrer to produce agar beads (100 to 200 µm). Then, to remove the mineral oil, we centrifuged (3000 × g, 15 min, 4 °C) the suspension of oil/beads. This approach allowed us to separate oil and agar bead phases and discard the surfacing oil by aspiration. Six washing steps with DPBS were performed and the agar beads were stored at 4 °C. Inoculum was determined by measuring the CFUs embedded within the agar beads after homogenization (gentleMACS Octo Dissociator with M Tubes, Miltenyi Biotec) and DBPS serial dilutions on 7H10 plates. CFUs were counted after five days of incubation at 37 °C. Mice were infected with an intratracheal injection of 10^5 CFU of *M. abscessus* (ATCC19977) embedded in agar beads, allowing persistence in the lungs of C57BL/6N immunocompetent mice with a sustained bacterial load. Fourteen days post-challenge, infected ($n = 3$) and uninfected ($n = 1$) mice (control mouse) were sacrificed, and lungs were collected for subsequent analyses. In addition, two mice were used to confirm the bacterial load at 14 days post challenges. At 14 days post-challenge, these mice were all infected, displaying a median bacterial load of 3.93×10^6 CFU, as previously published[27].

Animal studies were conducted according to protocols and adhering strictly to the Italian Ministry of Health guidelines for the use and care of experimental animals (IACUC N°1242) and approved by the San Raffaele Scientific Institute Institutional Animal Care and Use Committee (IACUC).

Histological examination

Murine lungs were removed, fixed in zinc formalin, and embedded in paraffin. Consecutive sections from the middle of the five lung lobes were used for Spatial Transcriptomics, Immunofluorescence examination and Acid-Fast Bacteria (AFB) staining for histology (Kinyoun method). Indirect immunofluorescence was performed using a rabbit polyclonal primary antibody ab905 (1:300 dilutions) with 1% BSA in PBS and the secondary Ab was Goat Anti-

Rabit IgG H&L (Alexa Flour ® 488) (ab150077). Host nuclei were stained with Hoechst 33342, Trihydrochloride. AFB staining was performed using a histology staining kit (Sigma-Aldrich) to detect acid-fast bacteria within histological tissue according to the manufacturer's instructions.

Immunofluorescence-stained slides were examined using DeltaVision™ Ultra microscope (GE Healthcare) at a magnification of 60x. The slides stained for AFB were examined using a Zeiss AxioImager M2m microscope with an AxioCam MRc5 at a magnification of 100x. Subsequent adjustments and bars were applied using ImageJ to ensure the accuracy of our results.

Bacterial target genes selection

The identification of target genes followed an analysis of transcriptome data derived from *M. abscessus* in vitro RNA sequencing, sourced from the online dataset curated by Schildkraut et al.[35] (GEO: GSE163621). This selection was based on examining gene expression levels within the untreated group in the in vitro standard growth condition. To prioritize genes for probe design, we quantified the gene expressions in terms of Transcripts Per Million (TPM) and ranked accordingly. Genes selected for probe design were *lsr2* (MAB_0545) and *rpoB* (MAB_3869).

Probe design

Probes were designed as described in the technical notes provided by 10x Genomics (Custom Probe Design for Visium Spatial Gene Expression and Chromium Single Cell Gene Expression Flex, CG000621) based on the reference sequence of *M. abscessus*[36]. In summary, distinctive 50-mer sequences were extracted from the specified target genes. Guided by the technical directives, sequences meeting specific criteria were isolated: those bearing a T at position 25, a CG% content ranging between 44–72%, and the absence of homopolymers with a length of 4.

Subsequently, the selected 50-mers underwent a comparative analysis against reference genomes using the BLAST tool. Sequences that exhibited matches to the *Mycobacterium abscessus* species while having no alignments to *Homo sapiens*, *Mus musculus*, or other bacterial species were selected. Within the context of each target gene, three sequences were chosen, ensuring a separation distance of at least 100 base pairs between each selected sequence. We ended up with a panel with three pairs of probes for each target bacterial mRNA (lsr2 and rpoB), with each probe containing a 25 bp sequence that is a reverse complement of the target mRNA sequence. Each probe is referred to as the left-hand side (LHS) or right-hand side (RHS) probe. The designed probes are listed here:

Gene name	Probe ID	Probe sequence
Lsr2 MAB_0545	MAB_0545_LHS_1	5'-CCTTGGCACCCGAGAATT CCAcaccgtcaacaccgaattcaacggt-3'
	MAB_0545_RHS_1	/5Phos/ctcgtcggcaggcgcttcgccg tcgAAAAAAAAAAAAA AAAAAAAAAAAAAAAAA-3'
	MAB_0545_LHS_2	5'-CCTTGGCACCCGAGAATT CCAttgtgcccgttcttacgtgcccact-3'
	MAB_0545_RHS_2	/5Phos/cgcggatcgccgcactctgc tcgcgAAAAAAAAAAAAAAA AAAAAAAAAAAAAA-3'
	MAB_0545_LHS_3	5'-CCTTGGCACCCGAGAATT CCAcacgacgcgcgtgctcgacccatgt-3'
	MAB_0545_RHS_3	/5Phos/agagagctgattacgcagcttctcc AAAAAAAAAAAAAAAAAA AAAAAAAAAA-3'
rpoB MAB_3869c	rpoB_LHS_1	5'-CCTTGGCACCCGAGAATT CCAtgccgttgatgatgaaggtgcccat-3'
	rpoB_RHS_1	/5Phos/atcggtcatcatcgggaaatcaccc AAAAAAAAAAAAAAAAAA AAAAAAAAAA-3'
	rpoB_LHS_2	5'-CCTTGGCACCCGAGAATT CCAtggtggtcacctgagccggattggt-3'
	rpoB_RHS_2	/5Phos/gccgcccaggcccagcttcttgttc AAAAAAAAAAAAAAAAAA AAAAAAAAAA-3'
	rpoB_LHS_3	5'-CCTTGGCACCCGAGAATT CCAggccttctccgcgacgacgacgtct-3'
	rpoB_RHS_3	/5Phos/ccggcgtcgatggcggcacgca attAAAAAAAAAAAAAAAAA AAAAAAAAAAAA-3'

Host-pathogen spatial transcriptomics

Formalin-fixed paraffin-embedded (FFPE) tissues were sectioned at 5 µm in thickness and attached to a Visium Spatial Gene expression slide. The tissue sections underwent hematoxylin and eosin (H&E) staining using the Visium Spatial Gene Expression protocol designed for FFPE tissue - Deparaffinization, H&E Staining, Imaging & Decrosslinking demonstrated protocol. Imaging was performed using a scanning tile microscope (Aperio AT2, Leica). Two consecutive slices of FFPE lung tissue were considered for both infected and uninfected mice (control mouse) (Supplementary Fig. 1).

Then, slides underwent tissue processing and library preparation following Visium Spatial Gene Expression for FFPE libraries demonstrated protocol. During Probe Hybridization (User guide CG000407), we introduced our customized probes according to 10x Genomics Technical note. We refined the Visium protocol to reinforce the Probe Hybridization and exploited the Diluted Permeabilization Enzyme B at 100X in Buffer EB. The same approach was also used for the control uninfected lungs. Libraries were sequenced on a Novaseq 6000 (Illumina) platform aiming at 25,000 reads pairs/spot. A report with a summary of the quality of the sequencing of both slices was provided (Supplementary Fig. 3). Sequencing data are available in the gene expression omnibus (GEO) under accession number GSE242471.

Count matrices generation. The Loupe Browser (version 6.0) was used to perform manual fiducial alignment and tissue selection to exclude spots corresponding to the airways. The output file in JSON format and the Fastq files underwent processing using the Spaceranger software from 10x Genomics (version 1.3.1) while adhering to default parameters. The reference dataset was modified accordingly for the detection of custom probes as stated in the 10x Genomics technical note (Custom Probe Design for Visium Spatial Gene Expression and Chromium Single Cell Gene Expression Flex, CG000621). The transcriptome reference was custom-made from space ranger 'mkref' using the Mouse reference dataset (mm10 Reference—2020-A), and ATCC 19977 *M. abscessus* genome assembly[36] (NC_010397.1). The Mouse Probe Set from 10X Genomics (Visium Mouse Transcriptome Probe Set v1.0), with custom *M. abscessus* probes appended to it, was used as the reference probe set in space ranger 'count'.

Quality control. After processing, the resultant filtered count matrices were imported and subjected to in-depth analysis using the R package Seurat (version 4.1.0)[37]. The filtered count matrices were separated into mouse count data and *M. abscessus* count data matrices. Spot level filtering was performed on the mouse count matrices to keep spots with at least 200 genes, and 250 UMIs (Supplementary Figs. 2 and 3). Gene level filtering was applied to omit genes that did not appear in at least 3 spots. *M. abscessus* UMIs were detected from four different sections, two with chronic infection and two uninfected controls (Supplementary Fig. 6).

Clustering analysis. The Seurat SCTransform function was applied to normalize the individual filtered count matrices (4 slices) and integrated in Seurat using SelectIntegrationFeatures and IntegrateData.

All the analysis were performed considering the four slices processed for Visium (supplementary Fig. 1). Initially, a Principal Component Analysis (PCA) was executed on integration genes, which allowed us to discern the

initial 30 principal components. These components were subsequently leveraged for UMAP dimensionality reduction and the establishment of a shared-nearest-neighbor graph. For the clustering of spots, the original Louvain algorithm was employed with a resolution parameter of 0.22. Clusters with more than 1% of the total spots were considered for the analysis.

Deconvolution analysis. A deconvolution step was performed using the annotated single-cell RNAseq reference dataset from Xu et al.[4] (GEO: GSE190225), accomplished through the RCTD algorithm from the spacexr package (version 2.0.1[28]). The deconvolution outputted cell-type weights matrices. After normalizing the cell-type weights at the spot level, the final matrix was saved as an assay Seurat object in addition to the gene counts assay. The parameters for the RCTD deconvolution were "max_cores = 2, test_mode = F, CELL_MIN_INSTANCE=6". The reference dataset for the convolution contained 12 cell types from Mouse lungs infected with *Klebsiella pneumoniae*.

Co-localization analysis. Spots demonstrating at least one read for the custom probe were designated as *M. abscessus* positive. The Differentially expressed (DE) genes distinguishing MABS+ spots from MABS− spots were obtained using 'FindMarkers' in Seurat, with default settings on the SCT normalized matrix. A nonparametric two-tailed Mann–Whitney U test was performed for the analysis. Both upregulated and downregulated DE genes were identified, with an adjusted p-value of 0.05. Cellular proportions were compared in each transcriptional cluster between MABS+ and MABS− spots for each chronic infection slice using a two-tailed Mann–Whitney U test. P values from comparisons similarly enriched for MABS+ or MABS− in both slices were then aggregated using Fisher's method for p-value aggregation. The threshold for the adjusted p-value, corrected with the false discovery rate, was set at 0.05.

Enrichment analysis. Enrichment analysis on Gene Ontology terms was performed using the MGI Gene Ontology dataset[38] and the R package ClusterProfiler (version 3.18)[39].

Statistical analysis. Comparisons of numerical variables among different groups were performed with a nonparametric one-tailed Mann–Whitney U test for two groups and the Kruskal–Wallis test for more than two groups, with a threshold of 0.05 for p-value adjusted with Bonferroni correction. In the case of comparing multiple different tests, Fisher's method for p-value aggregation was performed.

Reporting summary

Further information on research design is available in the Nature Portfolio Reporting Summary linked to this article.

Data availability

Sequencing data are available in the gene expression omnibus (GEO) under accession number GSE242471.

Code availability

Code is available in GitHub repository https://doi.org/10.5281/zenodo.13778548.

Received: 29 September 2023; Accepted: 20 September 2024;
Published online: 09 October 2024

References

1. Westermann, A. J. & Vogel, J. Cross-species RNA-seq for deciphering host-microbe interactions. *Nat. Rev. Genet* **22**, 361–378 (2021).
2. Gracia Villacampa, E. et al. Genome-wide spatial expression profiling in formalin-fixed tissues. *Cell Genom.* **1**, 100065 (2021).
3. Madissoon, E. et al. A spatially resolved atlas of the human lung characterizes a gland-associated immune niche. *Nat. Genet* **55**, 66–77 (2023).
4. Xu, Z. et al. Integrative analysis of spatial transcriptome with single-cell transcriptome and single-cell epigenome in mouse lungs after immunization. *iScience* **25**, 104900 (2022).
5. Cronan, M. R. et al. A non-canonical type 2 immune response coordinates tuberculous granuloma formation and epithelialization. *Cell* **184**, 1757–1774.e1714 (2021).
6. Galeano Nino, J. L. et al. Effect of the intratumoral microbiota on spatial and cellular heterogeneity in cancer. *Nature* **611**, 810–817 (2022).
7. Barrozo, E. R. et al. SARS-CoV-2 niches in human placenta revealed by spatial transcriptomics. *Med* **4**, 612–634.e4 (2023).
8. Bullman, S. et al. Analysis of Fusobacterium persistence and antibiotic response in colorectal cancer. *Science* **358**, 1443–1448 (2017).
9. McNulty, R. et al. Probe-based bacterial single-cell RNA sequencing predicts toxin regulation. *Nat. Microbiol.* **8**, 934–945 (2023).
10. Dar, D., Dar, N., Cai, L. & Newman, D. K. Spatial transcriptomics of planktonic and sessile bacterial populations at single-cell resolution. *Science* **373**, eabi4882 (2021).
11. Sounart, H. et al. Dual spatially resolved transcriptomics for human host-pathogen colocalization studies in FFPE tissue sections. *Genome Biol.* **24**, 237 (2023).
12. Saarenpaa, S. et al. Spatial metatranscriptomics resolves host-bacteria-fungi interactomes. *Nat. Biotechnol.* **42**, 1384–1393 (2024).
13. Sarfatis, A., Wang, Y., Twumasi-Ankrah, N. & Moffitt, J. R. Highly multiplexed spatial transcriptomics in bacteria. Preprint at *bioRxiv* https://doi.org/10.1101/2024.06.27.601034 (2024).
14. Milo, R. & Phillips, R. *Cell Biology by the Numbers* (2015).
15. Kang, Y. et al. Transcript amplification from single bacterium for transcriptome analysis. *Genome Res.* **21**, 925–935 (2011).
16. Vandereyken, K., Sifrim, A., Thienpont, B. & Voet, T. Methods and applications for single-cell and spatial multi-omics. *Nat. Rev. Genet* **24**, 494–515 (2023).
17. Johansen, M. D., Herrmann, J. L. & Kremer, L. Non-tuberculous mycobacteria and the rise of *Mycobacterium abscessus*. *Nat. Rev. Microbiol.* **18**, 392–407 (2020).
18. Nessar, R., Cambau, E., Reyrat, J. M., Murray, A. & Gicquel, B. Mycobacterium abscessus: a new antibiotic nightmare. *J. Antimicrob. Chemother.* **67**, 810–818 (2012).
19. Daley, C. L. et al. Treatment of nontuberculous mycobacterial pulmonary disease: an official ATS/ERS/ESCMID/IDSA clinical practice guideline. *Eur. Respir. J.* **56**, 2000535 (2020).
20. Lore, N. I. et al. The aminoglycoside-modifying enzyme Eis2 represents a new potential in vivo target for reducing antimicrobial drug resistance in *Mycobacterium abscessus* complex. *Eur. Respir. J.* **60**, 2201541 (2022).
21. Poerio, N. et al. Combined host- and pathogen-directed therapy for the control of *Mycobacterium abscessus* infection. *Microbiol. Spectr.* **10**, e0254621 (2022).
22. Khosravi, A. D., Hashemzadeh, M. & Rokhfirooz, P. Molecular identification of nontuberculous mycobacteria using the rpoB, argH and cya genes analysis. *AMB Express* **12**, 121 (2022).
23. Ferrell, K. C., Johansen, M. D., Triccas, J. A. & Counoupas, C. Virulence mechanisms of *Mycobacterium abscessus*: current knowledge and implications for vaccine design. *Front. Microbiol.* **13**, 842017 (2022).
24. Le Moigne, V. et al. Lsr2 is an important determinant of intracellular growth and virulence in *Mycobacterium abscessus*. *Front Microbiol.* **10**, 905 (2019).
25. Nish, S. & Medzhitov, R. Host defense pathways: role of redundancy and compensation in infectious disease phenotypes. *Immunity* **34**, 629–636 (2011).
26. Saliu, F. et al. Chronic infection by nontypeable Haemophilus influenzae fuels airway inflammation. *ERJ Open Res* **7**, 00614–02020 (2021).
27. Riva, C. et al. A new model of chronic *Mycobacterium abscessus* lung infection in immunocompetent mice. *Int. J. Mol. Sci.* **21**, 6590 (2020).

28. Cable, D. M. et al. Robust decomposition of cell type mixtures in spatial transcriptomics. *Nat. Biotechnol.* **40**, 517–526 (2022).
29. Sawyer, A. J. et al. Spatial mapping reveals granuloma diversity and histopathological superstructure in human tuberculosis. *J. Exp. Med.* **220**, e20221392 (2023).
30. Krausgruber, T. et al. Single-cell and spatial transcriptomics reveal aberrant lymphoid developmental programs driving granuloma formation. *Immunity* **56**, 289–306.e287 (2023).
31. Carow, B. et al. Spatial and temporal localization of immune transcripts defines hallmarks and diversity in the tuberculosis granuloma. *Nat. Commun.* **10**, 1823 (2019).
32. Dulberger, C. L. et al. Mycobacterial nucleoid-associated protein Lsr2 is required for productive mycobacteriophage infection. *Nat. Microbiol.* **8**, 695–710 (2023).
33. Lore, N. I. et al. IL-17A impairs host tolerance during airway chronic infection by *Pseudomonas aeruginosa*. *Sci. Rep.* **6**, 25937 (2016).
34. Nicola, F., Cirillo, D. M. & Lore, N. I. Preclinical murine models to study lung infection with *Mycobacterium abscessus* complex. *Tuberculosis* **138**, 102301 (2023).
35. Schildkraut, J. A. et al. RNA sequencing elucidates drug-specific mechanisms of antibiotic tolerance and resistance in *Mycobacterium abscessus*. *Antimicrob. Agents Chemother.* **66**, e0150921 (2022).
36. Kapopoulou, A., Lew, J. M. & Cole, S. T. The MycoBrowser portal: a comprehensive and manually annotated resource for mycobacterial genomes. *Tuberculosis* **91**, 8–13 (2011).
37. Hao, Y. et al. Integrated analysis of multimodal single-cell data. *Cell* **184**, 3573–3587.e3529 (2021).
38. Smith, C. L. & Eppig, J. T. The mammalian phenotype ontology: enabling robust annotation and comparative analysis. *Wiley Interdiscip. Rev. Syst. Biol. Med.* **1**, 390–399 (2009).
39. Yu, G., Wang, L. G., Han, Y. & He, Q. Y. clusterProfiler: an R package for comparing biological themes among gene clusters. *Omics* **16**, 284–287 (2012).

Acknowledgements

The authors thank Fiocchi A. and Guidotti L. (ANIMAL HISTOPATHOLOGY, IRCCS Ospedale San Raffaele, Milano, Italy) for the mouse histopathology preparations and the San Raffaele Microscopy facility (Alembic, Ospedale San Raffaele, Milano, Italy) for immunofluorescence images acquisition. In addition, the authors are grateful to Morgan GSK (Postdoctoral fellow, IRCCS Ospedale San Raffaele, Milano, Italy) for the critical reading and English grammar correction of the manuscript. Graphical abstract Created in BioRender. Tonon, G. (2024) BioRender.com/l98z407.

Author contributions

F.D., F.N., S.d.P., and N.I.L. conceptualized the study. S.d.P. and N.I.L. supervised the study. F.N., F.S., and N.I.L. performed processing protocols and in vivo experiments. F.N., F.G., F.S., and N.I.L. performed visium spatial library sequencing. Data was processed, curated, and visualized by F.D. and F.N. under the supervision of S.d.P. and N.I.L., and was analyzed by F.D. and S.d.P. The manuscript was drafted by F.D., F.N., S.d.P., and N.I.L. was reviewed and edited by F.G., G.T., and C.D.

Competing interests

The authors declare no competing interests.

Additional information

Supplementary information The online version contains supplementary material available at https://doi.org/10.1038/s42003-024-06929-5.

Correspondence and requests for materials should be addressed to Nicola I. Lorè.

Peer review information *Communications Biology* thanks Chairmandurai Arvindaraja, Lei Chen and the other, anonymous, reviewers for their contribution to the peer review of this work. Primary Handling Editors: Sridhar Mani and Tobias Goris.